Geomechanics and Engineering, *Vol. 34, No. 1 (2023) 17-27*
https://doi.org/10.12989/gae.2023.34.1.017

Calculation and field measurement of earth pressure in shield tunnels under the action of composite foundation

Chi Zhang[1a], Shi-ju Ma[*2], Yuan-cheng Guo[1b], Ming-yu Li[1c] and Babak Safaei[**3]

[1]*School of civil engineering, zhengzhou university, 100 science avenue, zhengzhou city, henan province, People's Republic of China*
[2]*School of civil engineering, zhengzhou university of Technology, 6 Yingcai Street zhengzhou city, henan province, People's Republic of China*
[3]*Department of Mechanical Engineering, Eastern Mediterranean University, North Cyprus via Mersin 10, Turkey*

(*Received August 4, 2022, Revised April 19, 2023, Accepted April 25, 2023*)

Abstract. Taking a subway shield tunnel in a certain section of Zhengzhou Metro Line 5 as an example, the field tests of shield cutting cement-soil monopile composite foundation were carried out. The load and internal force of the tunnel lining under the action of composite foundation were tested on-site and the distribution characteristics and variation laws of earth pressure around the tunnel under the load holding state of the composite foundation were analyzed. Five different load combinations (i.e., overburden load theory + q_0, Terzaghi's theory + q_0, Bierbaumer's theory + q_0, Xie's theory + q_0, and the proposed method (the combination of compound weight method and Terzaghi's theory) + q_0) were used to calculate the internal force of the tunnel structure and the obtained results were compared with the measured internal force results. The action mode of earth pressure on the tunnel lining structure was evaluated. Research results show that the earth pressure obtained by the calculation method proposed in this paper was more consistent with the measured value and the deviation between the two was within 5%. The distribution of the calculated internal force of the tunnel structure was more in line with the distribution law of field test data and the deviation between the calculated and measured values was small. This effectively verified the rationality and applicability of the proposed calculation method. Research results provided references for the design and evaluation of shield tunnels under the action of composite foundations.

Keywords: earth pressure; existing composite foundation; field monitoring; shield tunnel; theoretical calculation methods

1. Introduction

In geotechnical and civil engineering, safety estimation is crucial during various tunnel construction processes to avoid ground movements and ensure stability of tunnel face (Ngamkhanong *et al.* 2022, Keawsawasvong and Ukritchon 2022, Fraldi and Guarracino 2009). Shield method has been widely used in the construction of urban subways around the world. However, with the rapid development of cities, increasing cases of tunnel lines are approaching underground structures such as pile foundations, which impose additional loads on the tunnel lining structures and bring new scientific problems to tunnel structure design. It is an important part of tunnel design to be able to accurately evaluate the load action mode of tunnel structure. In tunnel design codes around the world, the calculation methods of vertical earth pressure load on the tunnel structure usually include: (a) ① Overburden load method (Tkaano, 2000); ② Terzaghi's method (Terzaghi 1936); ③ Bierbaumer's method (Bierbaumer 1913); and ④ Xie's method (Xie, 1964). However, there are many influencing factors in the determination of earth pressure value, which are not only related to stratum properties and tunnel lining structure form, but also affected by existing pile foundation, tunnel diameter, tunnel depth, grouting pressure and construction conditions (Li *et al.* 2015, Xiao *et al*. 2019). Field measurement data can comprehensively and effectively reflect the influence of various factors on earth pressure around the tunnel. Therefore, around the world researchers have collected and analyzed a large number of on-site tunnel earth pressure data (Kaya *et al*. 2022). Lai *et al.* (2022) investigated the stability of rectangular tunnels used in railway constructions based on finite element limit analysis (FELA) together with machine learning method. Shiau *et al*. (2022) established a stability model for elliptical tunnels by using Hoek–Brown failure design approach and FELA. Fathipour *et al*. (2020, 2021a, b) developed an FE model to anticipate the stability of retaining walls subjected to unsaturated conditions based on FELA and second-order cone programming (SOCP) method. Payan *et al*. (2022) explored the effects of non-associated flow rule on the geological stability of tunnels

∗Corresponding author, Ph.D.
E-mail: mashiju2010@126.com
**Corresponding author, Associate Professor
E-mail: babak.safaei@emu.edu.tr
[a]Ph.D. Student
[b]Professor
[c]Associate Professor

ISSN: 2005-307X (Print), 2092-6219 (Online)

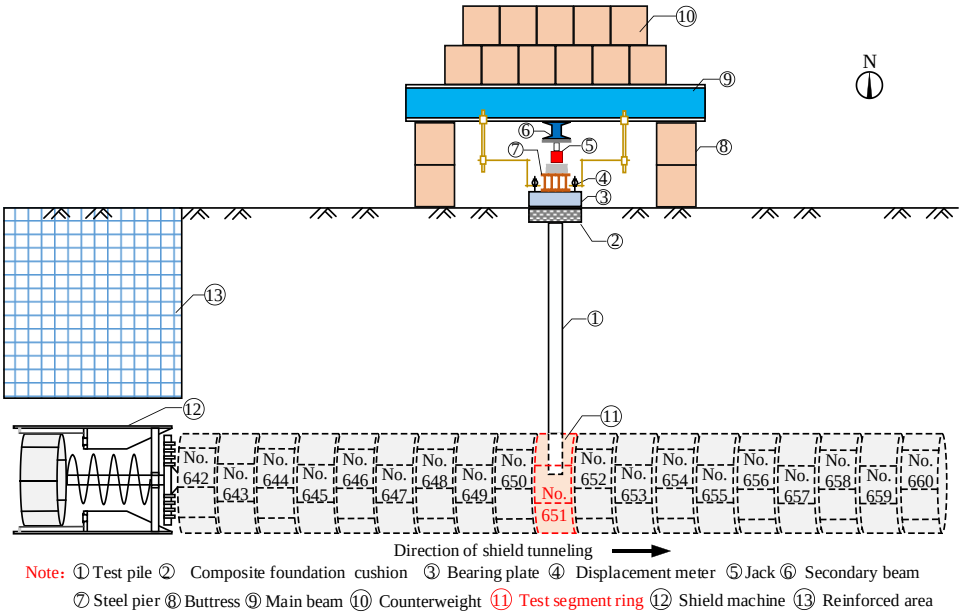

Fig. 1 Schematic diagram of shield cutting cement-soil single pile composite

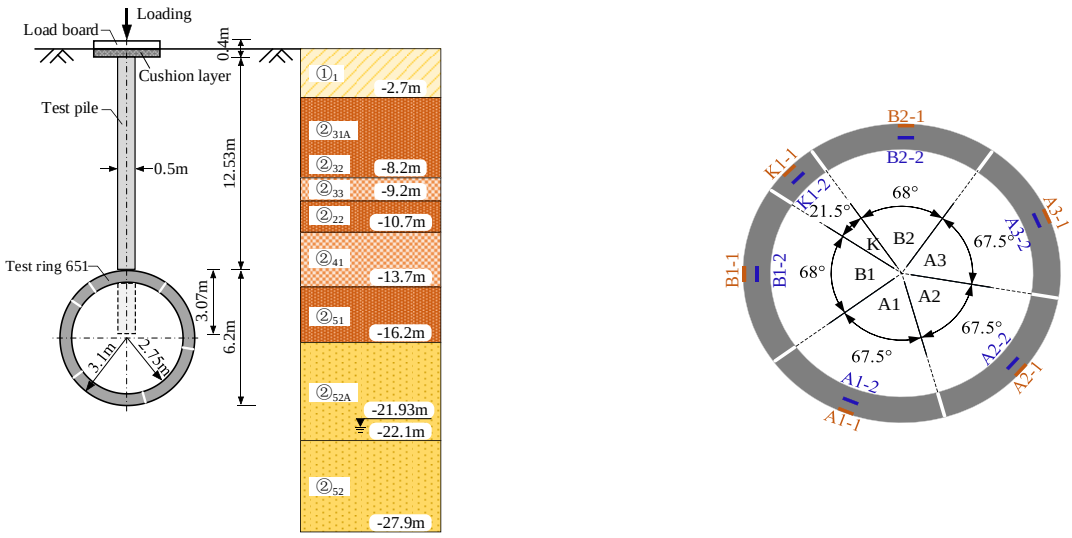

(a) Geological section of the test ring (b) Measuring point layout

Fig. 2 Geological section of the test ring and measuring point layout

using FELA and soil constitutive model. Also, Fathipour *et al.* (2022) studied the stability behaviors of active and passive lateral earth pressures based on unified effective stress approach incorporating SOCP under partially saturated porous conditions. Shiau and Keawsawasvong (2022) performed stability assessments of various two and three dimensional tunnel shapes subjected to different conditions based on Tresca approach and associate flow rule model.

To study the earth pressure acting on the shield tunnel, researchers have achieved fruitful results based on the analysis of field measured data. Mashimo (2003) evaluated the load effect of shield tunnels in gravel strata by means of field measurements. Koyama (2003) reviewed the development status of shield tunnels in Japan and studied the long-term earth pressure distribution law of tunnel lining structures. Atkinson (2013) analyzed the stress of segment structure by arranging earth pressure gauges on multiple strata sections. Using 3D numerical modeling analysis, Mukhtiar *et al.* (2022) found that the construction of shield tunnel adjacent to pile-raft foundation led to obvious differential settlement and flexural deformation of the building and the load distribution of pile body changed considerably. Leung (2011) introduced the influence law of earth pressure distribution on tunnel lining structure under the action of local contact loss between the tunnel lining and surrounding strata. Liu (2022) studied the distribution and evolution of supporting pressure and earth pressure during shield tunneling in a circular gravel layer and verified the reliability of test results through three-

Table 1 Physical and mechanical parameters of soil in various layers

No.	Layer	Soil gravity (kN/m^3)	Cohesion (kPa)	Internal friction angle (°)	Compressive modulus (MPa)	Thickness (m)
①$_1$	Qml	18.0	20.0	20.0	5.0	2.7
②$_{31A}$	Clayey silt	18.9	20.0	22.1	9.2	2.6
②$_{32}$	Clayey silt	19.4	19.9	21.2	8.5	2.9
②$_{33}$	Silty clay	19.6	29.5	16.4	5.7	1.0
②$_{22}$	Clayey silt	19.9	19.0	20.4	7.5	1.5
②$_{41}$	Silty clay	19.4	31.2	15.6	6.1	3.0
②$_{51}$	Clayey silt	20.2	19.3	20.7	8.7	2.5
②$_{52A}$	Fine sand	19.4	1.5	32.0	20.0	5.9
②$_{52}$	Fine sand	19.5	1.5	34.0	20.0	5.8

Table 2 Construction parameters of test ring excavation

Soil bin pressure (MPa)	Total thrust (kN)	Driving speed (mm/min)	Cutter-disk speed (rpm)	Cutter torque (kN·m)	Grouting pressure (MPa)	Grout amount (m^3)
0.065~0.085	21800~22300	8~18	1.08	3900~4550	3.6~5.2	7

dimensional numerical calculations. Li (2021) analyzed the evolution process and earth pressure law around the high-filled cut-and-cover tunnels with time so as to ensure the long-term stress safety of tunnel structures (Magbool and Tayeh 2021).

The above studies mostly aimed at shield tunnels in natural strata and there were few studies on the action mode of earth pressure of shield tunnels under the action of existing composite foundations (Zhao *et al.* 2022). Therefore, there is an urgent need for research on the effect of earth pressure around shield tunnels under the action of composite foundations. In this paper, by studying the distribution characteristics and earth pressure laws of shield tunnels under the action of composite foundations, five earth pressure calculation methods were used to obtain the internal force values of shield segments and compare them with measured internal force values to evaluate earth pressure under the action of composite foundations. Research results provided an important basis for subsequent tunnel designs under similar working conditions.

2. Engineering background and field test scheme

2.1 Engineering background

This paper is based on the background of the shield cutting group pile composite foundation crossing masonry structure project in a certain section of Zhengzhou Metro Line 5. In order to study the distribution and variation law of earth pressure around the tunnel under the working state (load-bearing state) of the composite foundation, a temporary parking lot 30 m away from the masonry structure house was selected to carry out the field tests of shield cutting cement-soil single pile composite foundation excavation (Ma, 2020) (Fig. 1). The tunnel lining segment had outer diameter of was 6.2 m, inner diameter of 5.5 m, thickness of 0.35 m, and width of 1.5m. It was prefabricated with C50 concrete and had an impermeability grade of P12. Each ring segment was composed of 1 capping block K + 2 adjacent blocks B + 3 standard blocks A. The segment was a double-sided universal wedge ring with a wedge shape of 40 mm. The assembly method was staggered seam assembly and the joints of segments were connected by curved bolts, including 16 M30 circumferential and 12 M30 longitudinal seam connecting bolts.

The thickness of the overlying soil on test ring (the ring No. 651 on the left line) was 12.53 m and groundwater level was lowered to -3.0 m below the tunnel arch bottom. The ratio of tunnel vault buried depth to lining structure outer diameter at monitoring section was about 2.05, which was a deep buried tunnel without hydraulic pressure. The stratum that the shield passed through was mainly silty clay layer, clay silt layer and fine sand layer. The geological profile of the test ring and positional relationship between the tunnel and composite foundation are shown in Fig. 2(a). The physical and mechanical parameters of the soil in each layer are given in Table 1 and the construction parameters of shield tunneling at test ring are summarized in Table 2.

2.2 Field test scheme

To study the change law of earth pressure and internal force of tunnel segment under the action of the existing composite foundation, in-situ tests were carried out on the imposed load and actual internal force of lining structure during the whole process of tunnel construction. During the test, in order to ensure the survival rate of the earth pressure cell, the installation of earth pressure cell was performed based on the method of burying the embedded parts. After the lining structure was poured, formed and maintained, embedded parts were found by chiseling and earth pressure box was bonded in the embedded parts with structural adhesive. One earth pressure cell and one reinforcing bar gauge were arranged on each segment of the test ring and 6 earth pressure cells and 6 reinforcing bar gauges were

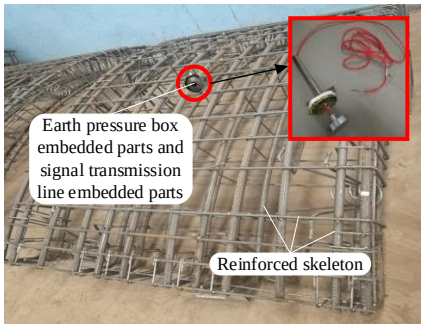

(a) Welding of embedded parts of earth pressure cell

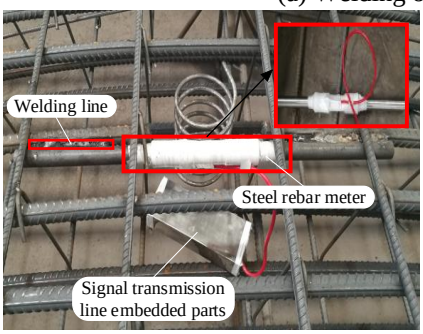

(b) Welding of steel rebar meter

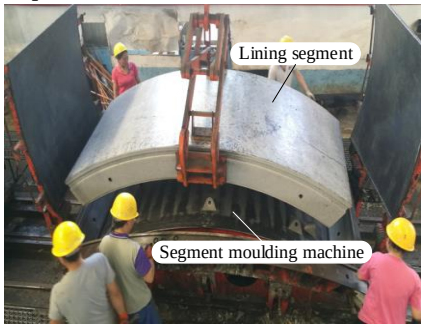

(c) Lining structure pouring and forming

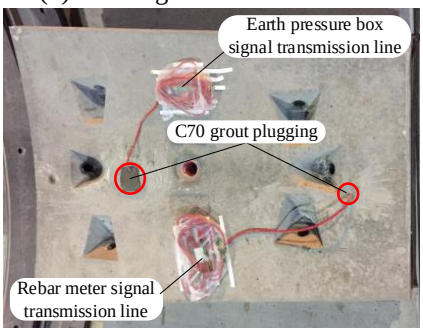

(d) Installation of earth pressure cells completed

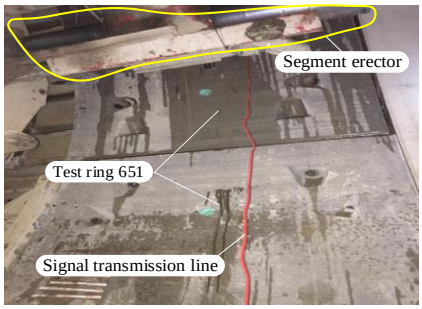

(e) On-site assembly of test ring (651 ring) segment

Fig. 3 Test instrument installation process

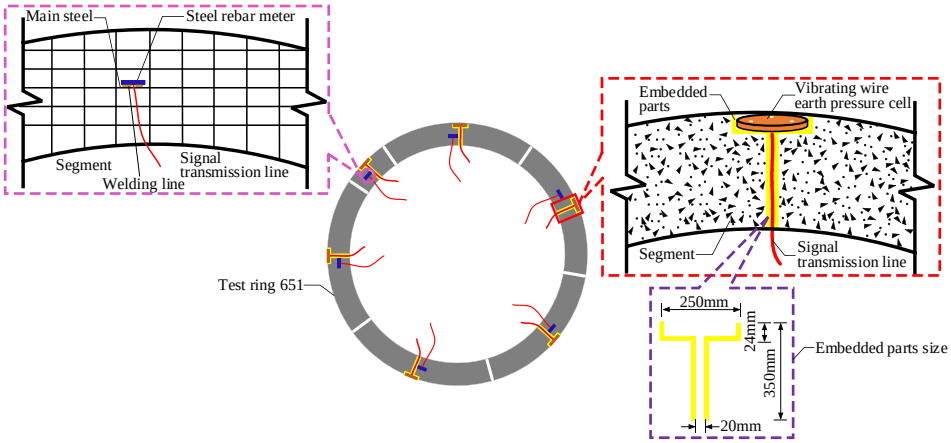

Fig. 4 Schematic diagram of the installation of steel rebar meter and earth pressure cell

embedded in the whole ring. The installation process of the original test piece is shown in Figs. 3(a)-4(e). Fig. 2(b) and Table 3 show the specific buried location and number of test originals. Fig. 4 illustrates the schematic diagram of the installation of rebar gauge and earth pressure cell.

3. Field measurement and analysis of earth pressure

Fig. 5 shows the time-history curve of the radial earth pressure of the tunnel under the action of composite foundation. According to the change of construction conditions

Table 3 Buried position of test original

Lining segment	Earth pressure cell numbering	Steel rebar meter numbering	Layout location
Adjacent block B2	B2-1	B2-2	0°
Standard block A3	A3-1	A3-2	67.75°
Standard blockA2	A2-1	A2-2	135.25°
Adjacent block A1	A1-1	A1-2	202.75°
Adjacent block B1	B1-1	B1-2	270.5°
Cap block K	K1-1	K1-2	315.25°

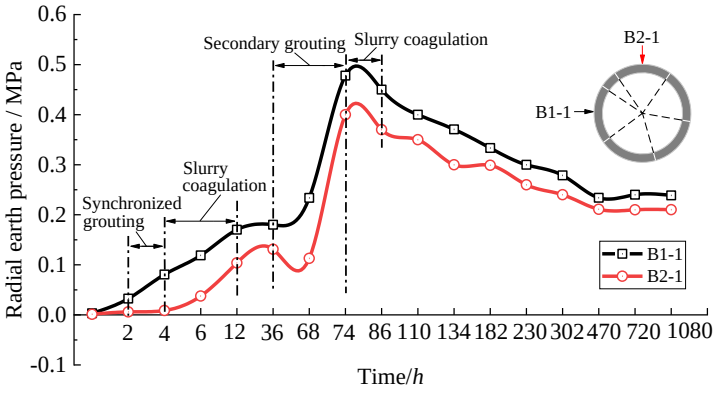

(a) Measuring point away from grouting well

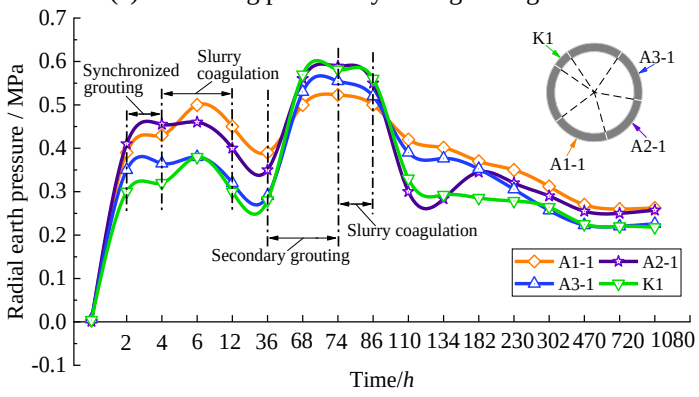

(b) Measuring point near the grouting well

Fig. 5 Time-history curve of tunnel radial earth pressure with time

with time, the change of radial earth pressure outside the test ring (the value measured by the earth pressure cell was the sum of the overburden earth pressure of the tunnel, the additional stress of the composite foundation and the influence of grouting pressure) could be divided into 4 stages for analysis as: lining structure detaching from the tail of the shield tunneling machine, synchronous grouting stage, secondary grouting stage and later stabilization stage.

It was seen from Fig. 5 that when lining structure was separated from shield tail, radial earth pressure on the outside of the lining structure increased to a certain extent due to the effect of the overlying earth pressure on the tunnel and the additional stress of composite foundation. Then, synchronous grouting stage was initiated. At this stage, lining structure was affected by the combined effect of the overlying earth pressure of the tunnel, additional stress of the composite foundation and grouting pressure, and radial earth pressure outside the tunnel was further increased. From Fig. 5(b), it was seen that the earth pressure monitoring points near the grouting hole were more obviously affected by grouting pressure. This showed that the radial earth pressure of the tunnel was rapidly increased during synchronous grouting and as the synchronous grouting slurry gradually began to condense, the radial earth pressure of the tunnel was decreased to some extent. During the secondary grouting stage, the radial earth pressure of each monitoring point outside the tunnel reached its peak value and its change showed a similar change rule to the radial earth pressure of the tunnel in synchronous grouting stage. As time passed, until the residual pile composite foundation above the tunnel reached a new state of stress balance and the overlying soil of the tunnel was gradually consolidated and reshaped to form a "pressure arch", radial earth pressure on the outside of the lining structure entered the following stage. In stable stage, the earth pressure value of each monitoring point tended to be stable.

Fig. 6 is the radar chart showing the changes in the radial earth pressure of the tunnel with the construction state under the action of the composite foundation. It was seen from Fig. 6 that after the lining structure of the test ring was separated from

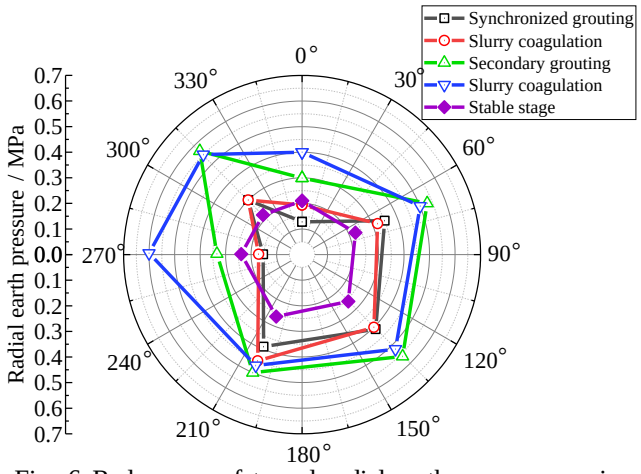

Fig. 6 Radar map of tunnel radial earth pressure varying with construction conditions

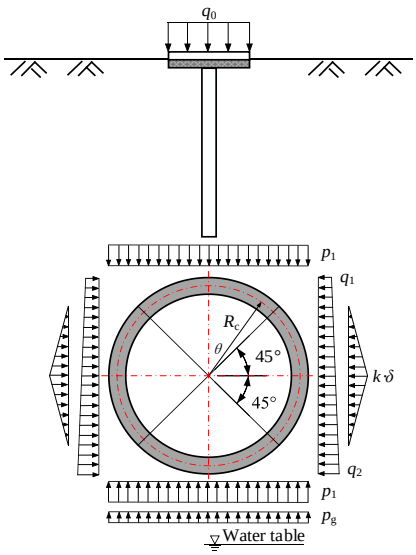

Fig. 7 Uniform method for calculation model

the shield tail, the overall radial earth pressure distribution of the tunnel was not uniform. After the test ring was separated from the shield tail, synchronous grouting was carried out to fill the building gap between the lining structure and stratum. At this time, the minimum radial earth pressure was 128 kPa at measuring point B2-1; that is, the adjacent lining segment B2. The maximum radial earth pressure was 410 kPa at A2-1 measuring point; that is, the standard lining segment A2. In order to reduce the influence of shield cutting pile effect on the settlement of composite foundation, synchronous grouting slurry on the outer side of the test ring lining structure was coagulated for 1 day and then the secondary grouting was carried out. The synchronous grouting slurry on the outside of the test ring lining structure was set for 1 day and then the secondary grouting was carried out. At this time, the radial earth pressure of each measuring point of the tunnel reached its maximum value and lining structure was greatly affected by grouting pressure. The radial earth pressure of the lining structure presented the order of arch waist > arch bottom > vault top. The maximum radial earth pressure was 600 kPa at the measuring point B1-1; that is, the standard lining segment B1. The minimum radial earth pressure was obtained to be 400kPa at B2-1 measuring point, which was adjacent to block B2. When the secondary grouting slurry was solidified for 15~40 days, radial earth pressure on the outside of the lining structure tended to be stable. Compared with the secondary grouting stage, the radial earth pressure on the outside of each measuring point of the tunnel was dropped by about 1/2 and its distribution shape was "horseshoe-shaped", which was relatively uniform. After stabilization, the order of the overall radial earth pressure of the tunnel was arch bottom > arch waist > arch top. At this time, the maximum radial earth pressure was 262 kPa at the measuring point A2-1; that is, the standard lining segment A1.

4. Evaluation of earth pressure: Theoretical calculation methods

In this paper, the load transfer effect of pile was not considered, the displacement effect of pile on soil was considered, and composite foundation reinforcement area was regarded as a composite soil mass. Composite weight method (Peng 2022) was used to recalculate the weight of composite soil and then, it was combined with Terzaghi theory to calculate earth pressure around the tunnel. In order to further study the magnitude and distribution law of earth pressure around shield tunnel under the action of composite foundation, the earth pressure around the tunnel was calculated by the method proposed in this paper, overburden load theory, Terzaghi's theory, Bill's theory and Xie's theory and the obtained results were compared with field measured values. The commonly used homogeneous ring method was used to calculate the internal force of the tunnel structure and its results were compared with field measured values.

4.1 Computational model

Homogeneous ring method, also known as uniform method (Guan 2012), was proposed in Japan around 1960 which was also one of the calculation methods widely used in tunnel design around the world. Based on the field test conditions in the present study, the calculation model could be simplified as shown in Fig. 7. In order to evaluate the load on the tunnel lining structure under the action of the composite foundation in load calculation, vertical earth pressure at the top of the tunnel was calculated by the following five combinations: ① Overburden load method + q_0, ② Terzaghi's method + q_0, ③ Bierbaumer's method + q_0, ④ Xie's method + q_0, and ⑤ the method developed in this research + q_0.

The calculation formula of overburden load method was

$$\sigma_v = \sum \gamma_i h_i + q_0 \tag{1}$$

where σ_v is vertical earth pressure at the top of the tunnel, kPa; γ_i is the weight of each layer of soil at the top of the tunnel and the floating weight below the groundwater level, kN/m^3; h_i is the thickness of each layer of soil at the top of the tunnel, m; and q_0 is ground additional overload, kPa.

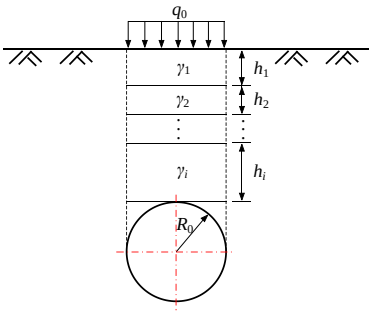

Fig. 8 Overburden load method computational model

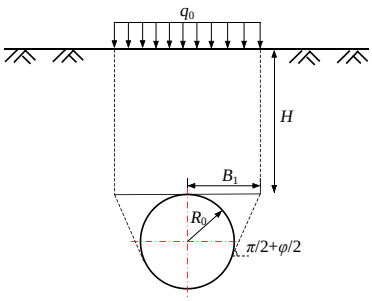

Fig. 9 Terzaghi's computational model

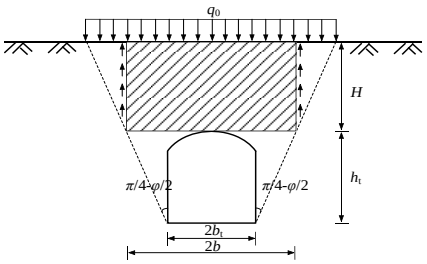

Fig. 10 Bierbaumer's computational model

The calculation equation of Terzaghi's method was stated as

$$\sigma_v = \frac{B_1(\gamma - \frac{c}{B_1})}{K_0 \tan\varphi}(1 - e^{-K_0 \tan\varphi \cdot H/B_1}) + q_0 e^{-K_0 \tan\varphi \cdot H/B_1} \quad (2)$$

where B_1 is 1/2 of the width of soil loose area, $B_1 = R_0 \cot(\frac{\pi/4+\varphi/2}{2})$, m; γ is the average weight of the soil at the top of the tunnel, kN/m^3; K_0 is lateral earth pressure coefficient; c is the cohesion of soil, kPa; φ is the internal friction angle of soil, °; H is the thickness of the soil layer at the top of the tunnel, m; R_0 is the outer diameter of the tunnel, m; and e is natural logarithm.

The calculation equation of Bierbaumer's method was stated as

$$\sigma_v = \gamma H\left[1 - \frac{H}{2b}K_1 - \frac{c}{\gamma b}(1 - 2K_2)\right] + q_0 \quad (3)$$

where $K_1 = \tan\varphi \tan^2(\frac{\pi}{4} - \frac{\varphi}{2})$, $K_2 = \tan\varphi \tan(\frac{\pi}{4} - \frac{\varphi}{2})$, $b = b_t + h_t \tan(\frac{\pi}{4} - \frac{\varphi}{2})$, the meaning of each parameter in the formula is the same as those in Eq. (2).

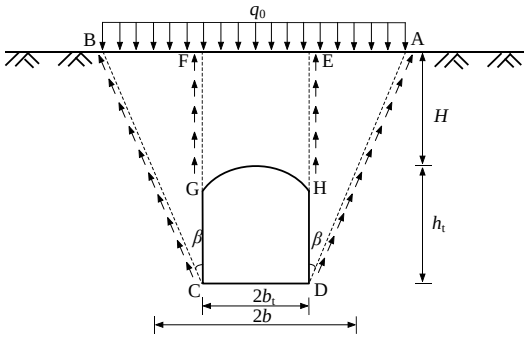

Fig. 11 Xie's computational model

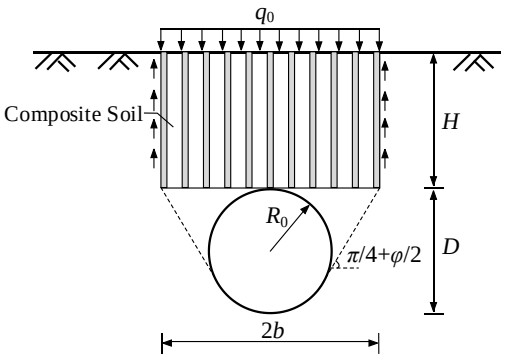

Fig. 12 The computational model developed in this research

The calculation equation of Xie's method was expressed as

$$\sigma_v = \gamma H + q_0 - \left[\gamma \frac{H^2}{2b_t} + 2q_0 \frac{H^2}{2b_t(H + h_t)}\right] K_0 \tan\theta \quad (4)$$

where θ is surrounding rock friction angle, ° and its value range was obtained as follows: when the surrounding rock grade was I, II, III, θ was 0.9φ; when the surrounding rock grade was IV, θ was 0.9 (0.7~0.9) φ; when the surrounding rock grade was V, θ was 0.9 (0.5~0.7) φ; and when the surrounding rock grade was VI, θ was 0.9 (0.3~0.5) φ; the meanings of the remaining parameters are the same as those in Eq. (3).

The calculation equation developed in this work paper method was

$$\sigma_v' = \frac{B_1(\gamma' - \frac{c'}{b})}{K_0' \tan\varphi'}(1 - e^{-K_0' \tan\varphi' \cdot H/b}) + q_0 e^{-K_0' \tan\varphi \cdot H/b} \quad (5)$$

where γ' is the average weight of soil at the top of the tunnel, kN/m^3. The meanings of the remaining parameters are the same as those in Eq. (2).

Horizontal earth pressure was calculated as

$$\sigma_h = \lambda \sigma_v \quad (6)$$

Calculation formula of radial earth pressure outside the tunnel was stated as

$$\sigma_r = \sqrt{\sigma_v^2 + \sigma_h^2} \quad (7)$$

The calculation parameters required for the above five tunnel earth pressure calculation models are summarized in Table 4.

Table 4 Model calculation parameters

Centroid radius R_c (m)	Segment thickness h (m)	Segment width t (m)	Lateral earth pressure coefficient λ	Cross-sectional area A (m^2)	Section moment of inertia I (m^4)	Segment Elastic Modulus E_c (Gpa)	Formation resistance factor k (MN/m^3)
2.925	0.35	1.5	0.5	0.525	0.005359	34.5	6.0

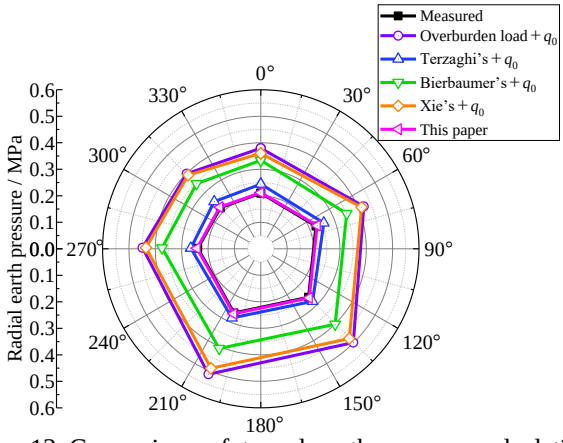

Fig. 13 Comparison of tunnel earth pressure calculation results under the influence of composite foundation

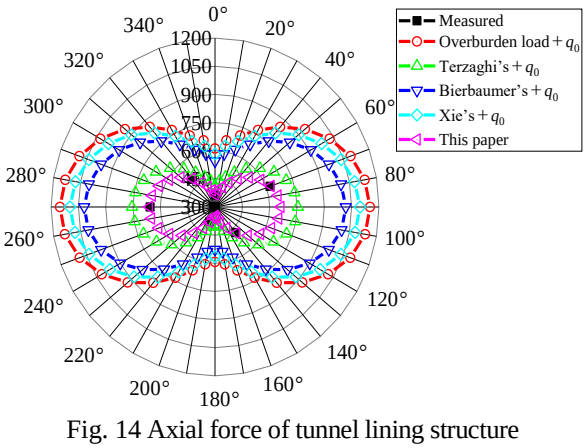

Fig. 14 Axial force of tunnel lining structure

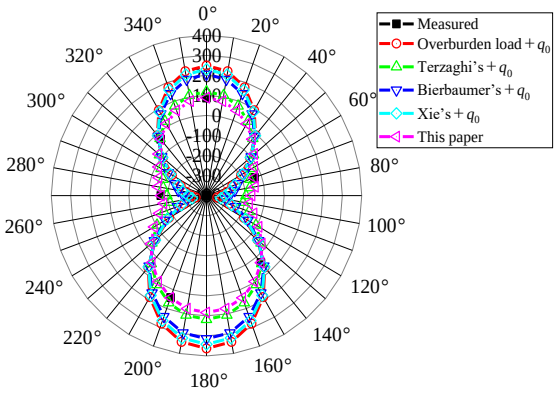

Fig. 15 Bending moment of tunnel lining structure

4.2 Calculation results and analysis

4.2.1 Earth pressure calculation results

Fig. 13 shows the comparison between the measured and theoretically calculated values of tunnel earth pressure after stabilization under the action of the composite foundation. It was seen from Fig. 13 that the calculated value of tunnel earth pressure after the stabilization of the earth pressure under the influence of the compound foundation shows that the theoretically calculated value of the Overburden load > Xie Jiaxiao's theoretical calculated value > Bierbaumer's theoretical calculated value > Terzaghi's theoretical calculated value > The algorithm calculated in this paper ≈ the measured value. The theory of overburden load considers the self-weight of the soil overlying the tunnel and the overloading of the composite foundation, and the calculated value of the soil pressure was about twice the measured value. Bierbaumer and Xie Jiaxiao theories took into account the dead weight of the overlying soil, the shearing action of soil and the overload of composite foundation, and the calculated value of earth pressure was about 1.5~1.7 times the measured value. Terzaghi theory took into account the self-weight of overlying soil, the shearing effect of soil, the arching effect of soil and the overload of composite foundation. The calculated value of earth pressure was about 1.15 times the measured value. The calculation method developed in this paper also took into account the self-weight of overlying soil, the shearing effect of soil, the arching effect of soil and the influence of composite foundation. The error between the calculated and measured values of earth pressure was within 5%. Therefore, the earth pressure value of the tunnel under the action of the composite foundation obtained by the earth pressure algorithm developed in this paper was closer to the measured value.

4.2.2 Internal force calculation results of lining structure

Figs. 14 and 15 show the comparison diagrams of the internal force results of the tunnel structure under the action of the composite foundation. It was seen from Figs. 14 and 15 that the distribution law of axial force and bending moment of tunnel structure calculated by the method developed in this paper was relatively consistent with the measured value. The calculated value showed that the theoretical calculating value of overburden load > Xie Jiaxiao's theoretical calculating value > Bierbaumer's theoretical calculating value > Terzaghi's theoretical calculating value > the calculated value obtained from the algorithm in the present paper ≈ the measured value.

It was seen from Fig. 14 that the axial force values of the tunnel were all positive values and the tunnel structure was in a state of compression. Axial force at the 90° position of the right arch waist and the 270° position of the left arch waist reached the maximum value and its value was the smallest at the 0° position of the vault and the 180° position of the arch bottom.

It was seen from Fig. 15 that the inner sides of the left and

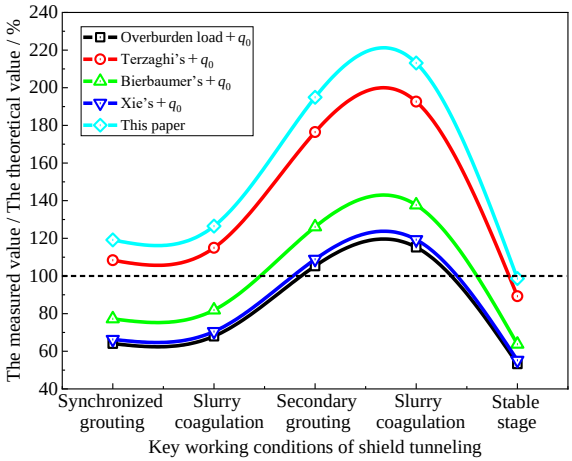

Fig. 16 Variation of the ratio of measured and theoretical values of earth pressure with shield construction

right arch waists of the tunnel were under tension and the outer sides were under compression and at the top and bottom of the tunnel, inner sides were under compression and the outer sides were under tension. According to the distribution law of the measured value of bending moment, it was seen that the calculation result obtained by the method proposed in this paper was in good agreement with the measured value of the bending moment of the tunnel structure. Therefore, the distribution law of the internal force of the tunnel structure obtained by the calculation method developed in this paper was more realistic and the deviation between the calculated and measured values was small, which verified the applicability and accuracy of the method proposed in this paper.

4.3 Calculation results and analysis

Fig. 16 shows the variation curve of the ratio of the measured value to the theoretical value of tunnel earth pressure with shield tunneling conditions under the action of the composite foundation. The measured value of the tunnel earth pressure also changed with shield tunneling conditions and the measured value of the tunnel earth pressure showed the law of dynamic nonlinear transformation. Earth pressure was obviously affected by construction disturbance effects such as synchronous grouting, secondary grouting, and grout condensation. In this paper, the dynamic stress process of the entire lining structure was divided into five stages according to the different working conditions of shield tunneling which included: separation from shield tail (synchronous grouting) stage, synchronous grouting slurry coagulation stage, secondary grouting stage, secondary grouting slurry condensation stage, and earth pressure stabilization stage.

The following is an analysis and evaluation of the calculation method of tunnel earth pressure under the influence of composite foundation in these five stages. The measured value of the tunnel earth pressure was close to the calculated value of the loose earth pressure of Terzaghi in separation from shield tail (synchronous grouting) and synchronous grouting slurry condensation stages and the measured value was 108%~115% of the calculated value of the loose earth pressure of Terzaghi. In secondary grouting and secondary grouting slurry setting stages, the measured value of the tunnel earth pressure was closer to the calculated value of overburden load and the measured value was 105%~115% of the calculated value of the overburden load. In stable stage, the measured value of the tunnel earth pressure was approximately equal to the calculated value of the earth pressure in this paper and the error between the two was within 5%.

Affected by the construction process of simultaneous grouting and secondary grouting, the measured value of tunnel earth pressure was much larger than the theoretically calculated value and the maximum value could reach 2.13 times the theoretically calculated value in this paper. However, the calculation method of tunnel earth pressure under the influence of composite foundation proposed in this paper could not perfectly consider the influences of various dynamic construction conditions on tunnel earth pressure and could only calculate tunnel earth pressure value in the stable stage of earth pressure more accurately.

Therefore, when the shield tunnel passed through the existing composite foundation, it was greatly affected by construction load and the load of the upper building. When designing segment lining structure, the most unfavorable working conditions should be considered to configure reinforcement. According to the calculation method proposed in this paper, reinforcing the lining segment could ensure the safety and reliability of the structure, and the corresponding reinforcing bars were more appropriate.

5. Conclusions

In this paper, the field measurement of the load and internal force of the tunnel lining under the action of the composite foundation was carried out and five different load combinations were used to evaluate the action mode of earth pressure of lining structures. The following conclusions were drawn:

- The field monitoring test of radial earth pressure around the tunnel under the action of the composite foundation was carried out and the distribution law of radial earth pressure around the tunnel structure under the action of the compound foundation was obtained. Earth pressure was greatly affected by grouting pressure (synchronous grouting and secondary grouting) in the early stage; after stabilization, the distribution pattern was "horseshoe-shaped", which was relatively uniform. The order of the overall soil pressure was arch bottom > arch waist > arch top.
- By comparing and analyzing different earth pressure calculation theories, i.e., overburden load theory, Terzaghi theory, Bierbaumer theory and Xie Jiaxiao theory, a new calculation method of earth pressure around the tunnel under the action of the composite foundation was proposed in this paper. The calculation method developed in this paper also considered the self-weight of overlying soil, the shearing effect of soil, the arching effect of soil and the influence of composite foundation. The deviation between the calculated and measured earth pressure values was within 5%.
- Using the uniform method commonly used in tunnel

design, the internal forces of tunnel structure were compared and analyzed. It was found that the internal forces of the tunnel structure calculated by overburden load theory, Terzaghi theory, Bierbaumer theory and Xie Jiaxiao theory were quite different from the measured values. These four traditional earth pressure calculation methods exaggerated load action, which significantly overestimated the calculated earth pressure value, which in turn caused the calculated value of the internal force of the tunnel structure to be too large, resulting in an increase in the amount of reinforcement in tunnel design. However, the earth pressure calculation method proposed in this paper had a high degree of agreement between the calculated and measured load and internal force of the tunnel structure, which could guide the design and calculation of tunnel lining structures more reasonably.

Acknowledgments

The research described in this paper was financially supported by the National Science Foundation of China (51508520) and remarkable assistance was received from China Railway 18th Engineering Bureau Group First Engineering Co. LTD.

Conflicts of interest

The authors declare that they have no conflicts of interest.

References

Bierbaumer. (1913), "Die dimensionerung des Tunelmauerwerks", Leipzig: Engelmann.

Bilotta, E. and Russo, G. (2013), "Internal forces arising in the segmental lining of an EPB bored tunnel", *J. Geotech. Geoenviron. Eng.*, **139**(10), 1765-1780. https://doi.org/10.1061/(ASCE)GT.1943-5606.0000906.

Fathipour, H., Bahmani Tajani, S., Payan, M., Jamshidi Chenari, R. and Senetakis, K. (2022), "Influence of transient flow during infiltration and isotropic/anisotropic matric suction on the passive/active lateral earth pressures of partially saturated soils", *Eng. Geol.*, **310**, 106883. https://doi.org/10.1016/j.enggeo.2022.106883.

Fathipour, H., Payan, M. and Jamshidi Chenari, R. (2021a), "Limit analysis of lateral earth pressure on geosynthetic-reinforced retaining structures using finite element and second-order cone programming", *Comput. Geotech.*, **134**, 104119. https://doi.org/10.1016/j.compgeo.2021.104119.

Fathipour, H., Payan, M., Jamshidi Chenari, R. and Senetakis, K. (2021b), "Lower bound analysis of modified pseudo-dynamic lateral earth pressures for retaining wall-backfill system with depth-varying damping using FEM-Second order cone programming", *Int. J. Numer. Anal. Method. Geomech.*, **45**(16), 2371-2387. https://doi.org/10.1002/nag.3269.

Fathipour, H., Safardoost Siahmazgi, A., Payan, M. and Jamshidi Chenari, R. (2020), "Evaluation of the lateral earth pressure in unsaturated soils with finite element limit analysis using second-order cone programming", *Comput. Geotech.*, **125**, 103587. https://doi.org/10.1016/j.compgeo.2020.103587.

Fraldi, M. and Guarracino, F. (2009), "Limit analysis of collapse mechanisms in cavities and tunnels according to the Hoek–Brown failure criterion", *Int. J Rock Mech. Min. Sci.*, **46**(4), 665-673. https://doi.org/10.1016/j.ijrmms.2008.09.014.

Guan, L.X. Translated. (2012), "Shield tunnel segment design", China Construction Industry Press, Beijing, China.

Kaya, M., Komur, A. and Gutsel, E. (2022), "Effect of aggregate mineralogical properties on high strength concrete modulus of elasticity", *Adv. Concrete Constr.*, **13**((6), 411-422. https:/doi.org/10.12989/acc.2022.13.6.411.

Keawsawasvong, S. and Ukritchon, B. (2022), "Design equation for stability of a circular tunnel in anisotropic and heterogeneous clay", *Undergr. Space*, **7**(1), 76-93. https://doi.org/10.1016/j.undsp.2021.05.003.

Koyama, Y. (2003), "Present status and technology of shield tunneling method in Japan", *Tunn. Undergr. Sp. Tech.*, **18**(2-3), 145-159. https://doi.org/10.1016/S0886-7798(03)00040-3.

Leung, C. and Meguid, M.A. (2011), "An experimental study of effect of local contact loss on the earth pressure distribution on existing tunnel linings", *Tunn. Undergr. Sp. Tech.*, **26**(1), 139-145. https://doi.org/10.1016/j.tust.2010.08.003.

Liu, X.R., Liu, D.S., Xiong, F., Han, Y., Liu, R., Meng, Q., Zhong, Z., Chen, Q., Weng, C. and Liu, W. (2022), "Experimental and numerical study on the stability of slurry shield tunneling in circular-gravel layer with different cover-span ratios", *Geomech. Eng.*, **28**(3), 265-281. https://doi.org/10.12989/gae.2022.28.3.265.

Li, S., Jianie, Y.C., Ho, I.H., Ma, L., Ning, G. and Wang, C. (2021), "Long-term behavior of earth pressure around a high-filled cut-and-cover tunnel", *Geomech. Eng.*, **26**(4), 311-321. https://doi.org/10.12989/gae.2021.26.4.311.

Li, X., Zhou, S.H., Gong, Q.M., *et al.* (2015), "Evaluation of earth pressure around a deeply buried metro shield tunnel with a large cross-section under high water pressure conditions", *Rock Soil Mech.*, **36**(5), 1415-1427.

Lai, V.Q., Shiau, J., Promwichai, T., Limkatanyu, S., Banyong, R. and Keawsawasvong, S. (2022), "Modelling soil stability in wide tunnels using FELA and multivariate adaptive regression splines analysis", *Model. Earth Syst. Environ.*, **1**, 1-16. https://doi.org/10.1007/s40808-022-01595-0.

Mashimo, H. and Ishimura, T. (2003), "Evaluation of the load on shield tunnel lining in gravel", *Tunn. Undergr. Sp. Tech.*, **18**(2-3), 233-241. https://doi.org/10.1016/S0886-7798(03)00032-4.

Mukhtiar, A.S., Naeem, M., Aftab, H.M. and Dildar, A.M. (2022), "Responses of high-rise building resting on piled raft to adjacent tunnel at different depths relative to piles", *Geomech. Eng.*, **29**(1), 25-40. https://doi.org/10.12989/gae.2022.29.1.025.

Ma, S.J., Li, M.Y., Guo, Y.C. and Safaei, B. (2020), "Field test and research on shield cutting pile penetrating cement soil single pile composite foundation", *Geomech. Eng.*, **23**(6), 513-521. https://doi.org/10.12989/gae.2020.23.6.513.

Magbool, H. and Tayeh, B. (2021), "Influence of the roughness and moisture of the substrate surface on the bond between old and new concrete", *Adv. Concrete Constr.*, **12**(1), 33-45. https://doi.org/10.12989/acc.2021.12.1.033.

Ngamkhanong, C., Keawsawasvong, S., Jearsiripongkul, T., Cabangon, L.T., Payan, M., Sangjinda, K., Banyong, R. and Thongchom, C. (2022), "Data-driven prediction of stability of rock tunnel hrading: An application of machine learning models", *Infrastructures*, 7(11), 148.

Payan, M., Fathipour, H., Hosseini, M., Jamshidi Chenari, R. and Shiau, J.S. (2022), "Lower bound finite element limit analysis of geo-structures with non-associated flow rule", *Comput. Geotech.*, **147**, 104803. https://doi.org/10.1016/j.compgeo.2022.104803.

Peng, F., Ma, S.J., Li, M.Y. Fu, K. (2022), "Stress performance evaluation of shield machine cutter head during cutting piles

under masonry structures", *Adv. Civil Eng*. https://doi.org/10.1155/2022/4111637.

Shiau, J. and Keawsawasvong, S. (2022), "Producing undrained stability factors for various tunnel shapes", *Int. J. Geomech*., **22**(8), 06022017. https://doi.org/10.1061/(ASCE)GM.1943-5622.0002487.

Shiau, J., Keawsawasvong, S. and Seehavong, S. (2022), "Stability of unlined elliptical tunnels in rock masses", *Rock Mech. Rock Eng.*, **55**(11), 7307-7330. https://doi.org/10.1007/s00603-022-02996-4.

Tkaano, Y.H. (2000), "Guidelines for the design of shield tunnel lining", *Tunn. Undergr. Sp. Tech.*, **15**(3), 303-331. https://doi.org/10.1016/S0886-7798(00)00058-4.

Terzaghi K. (1936), "Stress distribution in dry and in saturated sand above a yielding trap-door", *Proceedings of the 1st International Conference on Soil Mechanics and Foundation Engineering*, Cambridge, Massachusetts.

Xie, J.Z. (1964), "Formation pressure of shallow tunnels", *Chinese J. Civil Eng.*, **10**(6), 58-70.

Xiao, M.Q., Feng, K., Li, C., *et al.* (2019), "A method for calculating the surrounding rock pressure of shield tunnels in compound strata", *Chinese J. Rock Mech. Eng.*, **38**(9), 1837-1847.

Zhao, W., Zhong, K., Chen, W. and Xie, P. (2022), "A quasi-static finite element approach for seismic analysis of tunnels considering tunnel excavation and P-waves. Earthquakes and Structures", *Adv. Concrete Constr*., **22**(6), 549-559. https://doi.org/10.12989/acc.2022.22.6.549.

GC